Nucleation and growth behaviour of chunky graphite

Dr Haruki Itofuji* and Ayumi Masutani
Technical Development Sec., Ube Steel Co., Ltd., 1978–19 Okinoyama, Kogushi, Ube City Yamaguchi Pref., 755–0067 Japan

The nucleation and growth behaviour of chunky graphite in heavy section ductile cast irons was studied. The microstructure in the quenched samples during solidification was observed using optical microscopy and EPMA. Only spheroidal graphite was observed as the initial form of graphite at the early stage of the solidification. When the growth of the graphite nodules stopped during solidification, chunky graphite began to nucleate at the interfacial sites around the solidification front of the austenite and grow at the thin liquid channel in austenite. During this growth, the advancing end came into contact with the residual liquid iron through the thin liquid channel. Spheroidal graphite is not directly related to the nucleation and growth of chunky graphite. In this study, the Site Theory is used as one explanation of the nucleation and growth mechanism.

Introduction

The formation of chunky graphite at the thermal centre of heavy sections is the most incomprehensible phenomenon in the production of ductile iron castings. It has already been shown that the elements such as Ce[1–7], Si[7–9], Ca[4,10–12], Ni[7–9,13], and Cu[7,9] and Al[7] promote the formation of chunky graphite when they exceed a certain content. On the other hand, it has been also shown that the existence of elements such as Pb[7,14–16], Sb[4,7,9,12,15,17–19], As[20], Bi[15], Sn[5,7,8], B[7,9] and Cu[5] suppress the formation of such graphite. In practice, Sb is added as the most effective countermeasure to prevent the formation of chunky graphite but it is still not a reliable countermeasure. The solidification mechanism of chunky graphite is still not understood, although many researchers have tried to make it clear.

The typical microstructure and the three dimensional appearance of chunky graphite are shown in Figs 1[21] and 2,[22] respectively. The microstructure looks different from the other types of graphite in magnesium-treated irons, such as spheroidal and CV graphite. However, the fundamental substructure has been found to be the same among those graphites.[22] It has also been shown that inclusions at the growth front of the austenite dendrite skeleton affect the nucleation and growth of chunky graphite[22].

In this paper, the nucleation and growth behaviour of chunky graphite will be clarified through observation of the microstructure of samples quenched during a prolonged solidification, using optical microscopy and EPMA. In this study, the Site Theory[23] has been used to understand the nucleation and growth mechanism of chunky graphite and the author would welcome other interpretations of the data.

Experimental procedure

The experimental apparatus is shown in Fig. 3. The base metal was melted using a 10 ton low frequency induction furnace and then treated with Fe-Si-5.5%Mg and Fe-75%Si using the sandwich method. After the Mg reaction finished, liquid iron of about 1.2 kg was taken from the ladle using a preheated graphite spoon, and it was poured into the graphite crucible preheated to 1250° in the experimental SiC furnace. The rest of the liquid iron was poured into the mould. To adjust the chemical composition of the liquid iron for the easy precipitation of chunky graphite, 50% Ce mish metal and Fe-75%Si were set in the preheated graphite crucible just before pouring. The liquid iron was stirred using a preheated silica tube, soon after pouring. Then, lids were immediately put on the graphite crucible and the experimental furnace respectively. Since the lid for the graphite crucible directly touched the liquid iron, it was also preheated at 1250°C in the experimental SiC furnace. The whole operation of sampling was conducted within 10 seconds. The required chemical composition in the graphite crucible was 3.45C, 2.80Si, 0.20Mn, <0.050P, <0.015S, 0.020–0.040Ce, 0.050%Mg.

Several trials were conducted to find the optimum condition for chunky graphite precipitation in the experimental SiC furnace. As a result, the precipitation of chunky graphite was found to be favoured when both the time duration from sampling to solidification start, and the solidification time itself was long. In the experimental furnace, each liquid iron sample was cooled and solidified according to the schedule in Fig. 4, using the furnace controller. Each liquid iron sample was quenched in a water bath at selected intervals during the controlled solidification. The microstructure of each quenched sample was observed using optical microscopy in its entirety and in the location near the thermocouple. EPMA was used for the detailed observation. The samples were etched with 5% nital. Chemical analysis was conducted at the middle layer near the thermocouple in each quenched sample, according to JIS G 1211, 1212, 1215 and 1257.

*Author for correspondence
e-mail: h-itofuji@mx5.tiki.ne.jp

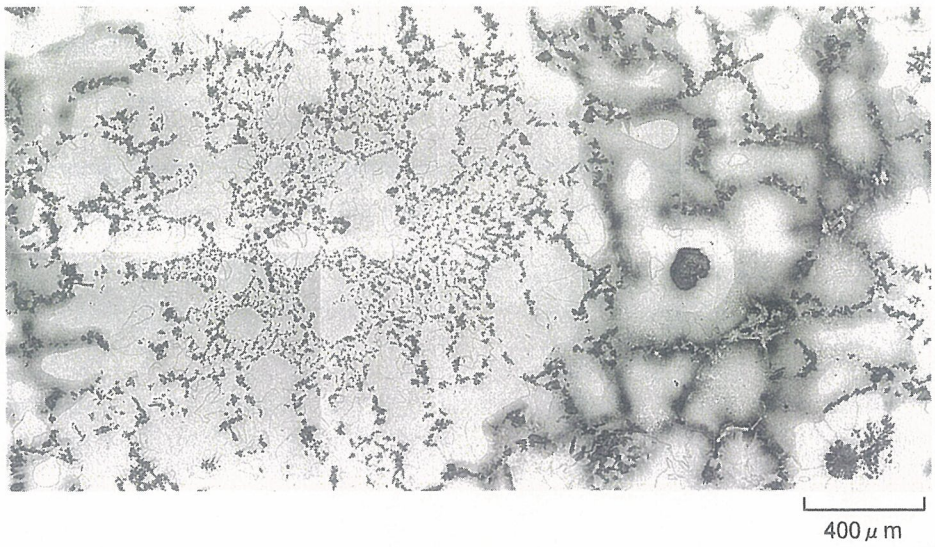

Fig. 1 Microstructure of chunky graphite layer at thermal centre of 230 mm wall thickness (2% nital etch)[21]

Results

The cooling curve, of the chunky graphite structure under controlled solidification, is shown in Fig. 5. The quenching points were selected at the critical stages on the cooling curve, They are shown by the arrows labelled with numbers in Fig. 5. At first, the master cooling curve was drawn from sample No. 5. Other liquid irons were then quenched into water in the count-down order of 4, 3, 2 and 1 during their controlled solidification. Good reappearance was obtained among the cooling curves. The average time duration from the sampling to the solidification start in liquid irons was about 35 minutes. Here, the solidification start was supposed to be equal to the beginning of the primary graphite precipitation. The temperature history of each liquid iron until quenching is shown in Table 1. When chunky graphite formed, the γ-graphite eutectic temperature was close to the equilibrium state and the recalescence became quite small, at about 4 °C. The chemical composition of each quenched sample is shown in Table 2. The carbon equivalent of all the liquid iron in the crucible was controlled at 4.4–4.5%. The carbon equivalent in the quenched samples, however, decreased toward the equilibrium eutectic composition in samples No. 3, 4 and 5. The observed results of the quenched microstructure are described below. In the quenched microstructure, the residual liquid iron was observed always as ledeburite. However, the austenite shell and dendrite were observed mostly as lens martensite and rarely as fine pearlite.

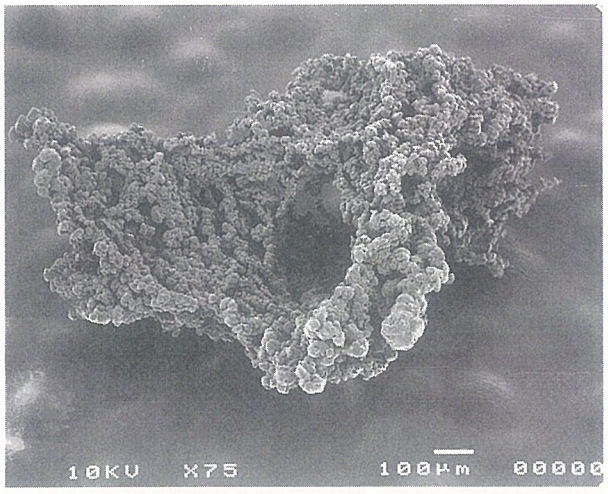

Fig. 2 SEM photo of chunky graphite cell extracted from the micro specimen.[22] The optical microstructure of the specimen is shown in Figure 1

Formation process

Even if the conditions of liquid iron and cooling led to the chunky graphite structure, a tiny graphite nodule (sphere graphite) under 10 μm was directly precipitated in the liquid iron as primary graphite at an early stage of the solidification, similar to spheroidal and CV graphite iron. However, austenitic dendrites also precipitated simultaneously in the liquid iron, even in the hyper eutectic solidification. This was a typical phenomenon in the solidification of iron with chunky graphite. The microstructure of sample No. 1 is shown in Fig. 6.

As the solidification progressed, the number of sphere graphite nodules increased, the sphere graphite was surrounded with austenite shell, and austenite dendrite grew further. The sphere graphite nodules were bigger in size but there were fewer nodules when compared to spheroidal and CV iron at the similar quenching point. In specific terms, the nodules were more than five times the size and the number of sphere graphite nodules was less than one third. Liquid iron sample no. 2 was quenched before the recalescence reached the maximum. The microstructure of this sample is shown in Fig. 7. It shows that many sphere graphite nodules surrounded with austenite shell had a dual substructure but sphere graphite nodules in liquid

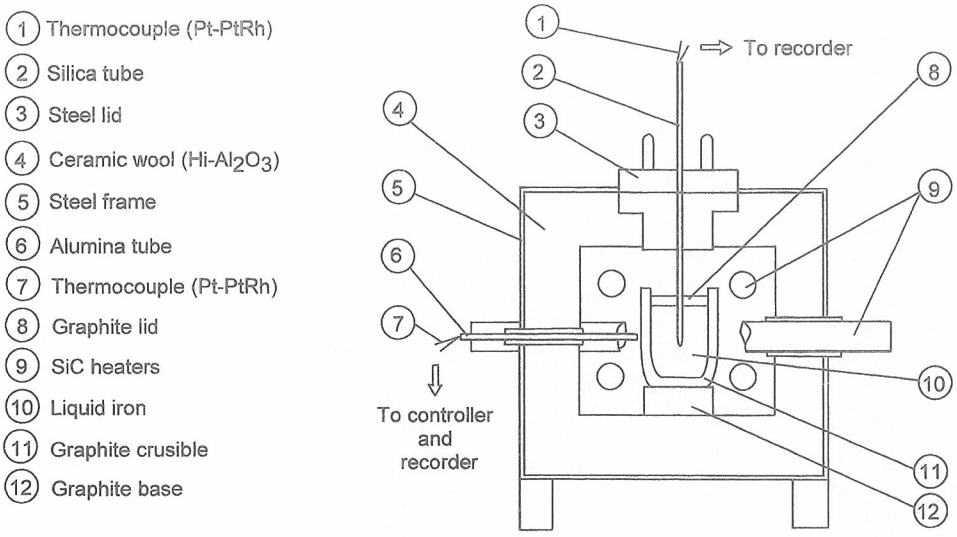

Fig. 3 Experimental SiC furnace for simulative solidification (effective inside dimension = 150 × 150 × 180 mm)

iron did not. This indicates that nodules in the inner and the outer ring followed a different growth process history.

In samples No. 1 and 2, the precipitation of granular-like graphite was observed around the growth front of the austenite.

Liquid iron 3 was kept for one hour at 1150°C in the furnace and then quenched into the water bath. The microstructures of sample No. 3 are shown in Fig. 8. In this sample, a large graphite nodule of 150–200 μm in diameter was observed in the austenite shell. The nodule was already isolated from the residual liquid iron; the thin liquid channel connecting spheroidal graphite to residual liquid iron was already closed. A large amount of austenitic dendrite was observed in the residual liquid iron. Granular-like graphite was also observed around the growth front of these austenites. On the other hand, the precipitation of chunky graphite began to be observed at this point. The precipitation patterns were divided into two. One showed that chunky graphite precipitated at the site between the austenite shell with the large graphite nodule and the austenitic dendrite (Fig. 8a). The second site was among the austenite shells (Fig. 8b).

Liquid iron 4 was kept for two hours at 1150 °C in the furnace and then quenched into the water bath. The microstructures of sample No. 4 are shown in Fig. 9. In this sample, the growth of chunky graphite was dominant. However, it seemed that the large graphite nodule had hardly changed in its morphology from the sample No. 3. At this stage, granular-like graphite was no longer observed around the growth front of the austenite

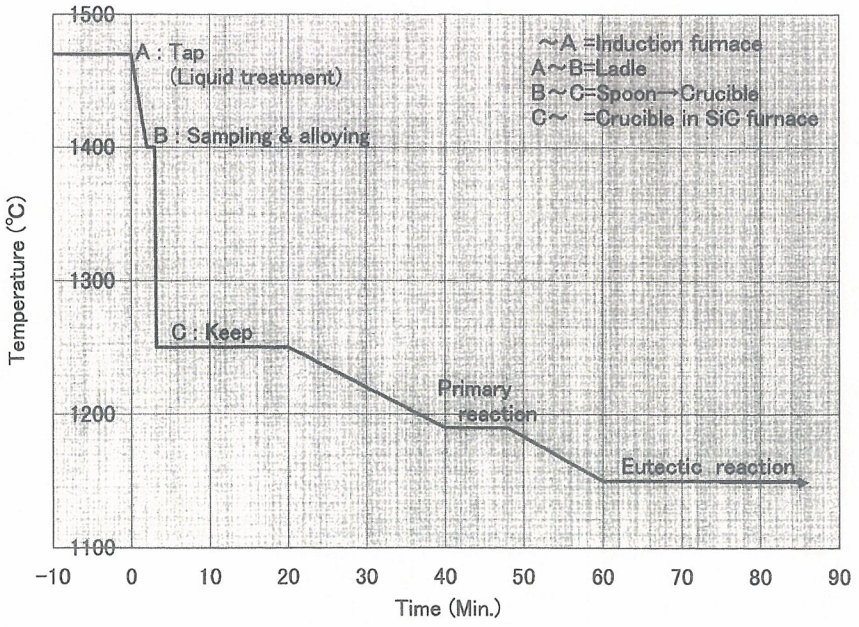

Fig. 4 Time and temperature schedule for liquid iron to form chunky graphite structure

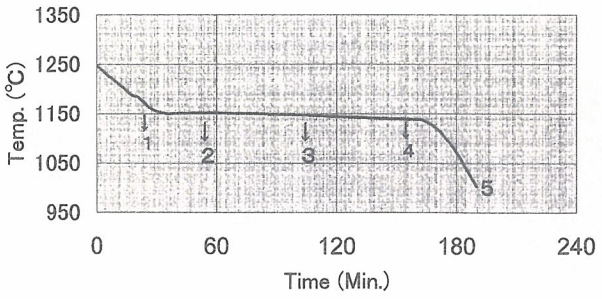

Fig. 5 Cooling curve of iron with chunky graphite and quenching points of liquid irons during the solidification

shell and dendrite. However, an additional precipitation pattern of chunky graphite was now observed among austenite dendrite arms (Fig. 9-b).

During the growth, the growth front of the chunky graphite came into contact with the residual liquid iron through the liquid channel (Fig. 10). N. Yingyi[6] and J. Zhou[9] have also reported this.

Figure 11 shows the microstructure of the sample completely solidified in the furnace. The shape, the size and the number of large graphite nodules observed in samples No. 3, 4 and 5 were almost identical. This means that the growth of graphite nodules had almost saturated when the chunky graphite began to nucleate and grow.

Through the whole observation, no chunky graphite connecting directly to a large graphite nodule was observed. They had no direct relationship to each other in the formation process. The chunky graphite began to nucleate after the growth of the large graphite nodules had almost stopped, as verified above.

Nucleation site

The areas around the growth front of the austenite shell with large graphite nodules and the austenite dendrite were observed in detail to find the nucleation site of the chunky graphite. (It has already been shown in Fig. 6 that precipitation begins in these areas). Granular-like graphite, which is the initial form of chunky graphite, was frequently observed at the austenite-inclusion interface. Inclusions connecting to granular-like graphite at the growth front of austenite shell and dendrite could be divided into two types by their colour and morphologies (Fig. 12). Each type was analysed by Energy Dispersive X-ray Spectrography (EDS). The results showed that one was light brown and Fe-Mg-Si-P-S-Ca-RE system, and that another was gray and Fe-Mg-Al-Si-tr.(S, Ca, RE) system (Fig. 13). The sites of the chunky graphite nucleation are described below;

1 among austenite shell
2 between austenite shell and austenite dendrite
3 around austenite dendrite
4 between austenite dendrite arms

The examples of the chunky graphite nucleation at the austenite-inclusion interface are shown in Figs 14 and 15. The growth front came into direct contact with the residual liquid iron, in the same way as shown in Fig. 10.

J. Zhou[9] has reported that chunky graphite nucleates near austenite dendrite but not in liquid iron. N. Yingyi[6] has reported that chunky graphite formed at the liquid iron-austenite interface and that RE, Mg, S, O, etc. were enriched at the interface. Neither, however, describes details on the nucleation and growth.

Discussion

Role of magnesium for the nucleation and growth of chunky graphite

According to the Site Theory, magnesium gas bubbles provide a site for graphite nucleation and growth and then affect the morphology of austenite shell. Magnesium does not directly influence the fundamental growth behaviour of the hexagonal graphite crystal structure, but a Mg gas bubble can influence the graphite substructure.

The nucleation and growth mechanism of spheroidal, CV and chunky graphite during the solidification can be schematically illustrated as shown in Fig. 16. This illustration indicates that spheroidal, CV and chunky graphite in part have a common process of nucleation and growth, and that they have the polycrystal substructure[22,23] in

Table 1 Temperature change of each liquid iron from tapping to quenching (°C)

			Graphite crucible					
			Initial after		Eutectic reaction		Recalescence	
Sample	Induction furnace	Ladle	sampling	Primary reaction	Min.	Max.	ΔT	Quenching
1	1461	1406	1272	1177	–	–	–	1165
2	1457	1396	1256	1170	1157	–	–	1158
3	1448	1392	1230	1180	1150	1154	4	1153
4	1468	1405	1260	1189	1150	1154	4	1153
5	1550	1516	1310	1183	1154	1158	4	As cast

Table 2 Chemical composition near the thermocouple at the middle layer of each quenched sample

Sample	Chemical composition (Mass%) C	Si	Mn	P	S	Ca	Ce	Mg	CE
1	3.42	2.94	0.30	0.046	0.005	0.0037	0.047	0.035	4.40
2	3.42	2.88	0.15	0.048	0.005	0.0021	0.037	0.029	4.38
3	3.29	2.91	0.14	0.046	0.006	0.0012	0.022	0.035	4.26
4	3.30	2.78	0.22	0.036	0.009	0.0004	0.031	0.042	4.23
5	3.31	2.79	0.19	0.042	0.014	0.0053	0.020	0.026	4.24

$CE = C + 1/3Si$

Table 2 continued

Sample	Cu	Ni	Cr	Mo	Ti	Sn	Al	Pb	As	Bi	Sb	Zn	V	Nb
1	0.02	0.02	0.10	0.08	0.005	0.002	0.020	0.000	0.000	0.000	0.001	0.002	0.001	0.001
2	0.02	0.02	0.07	0.00	0.006	0.002	0.018	0.000	0.000	0.000	0.001	0.002	0.001	0.001
3	0.02	0.02	0.06	0.00	0.006	0.002	0.022	0.000	0.000	0.000	0.001	0.003	0.001	0.001
4	0.02	0.03	0.09	0.04	0.005	0.004	0.018	0.000	0.000	0.000	0.001	0.001	0.001	0.001
5	0.06	0.03	0.09	0.00	0.005	0.003	0.020	0.000	0.000	0.000	0.001	0.025	0.001	0.001

common. Their mechanism can be, therefore, explained by a single theory. Graphite fills up a gas bubble and forms a tiny graphite nodule less than 10 μm (sphere graphite) in liquid iron.[23,24] The sphere graphite is then surrounded with austenite shell. Spheroidal and CV graphite start to grow from sphere graphite in the austenite shell. Chunky graphite has no direct relationship with the graphite nodule on its nucleation and growth. Chunky graphite nucleates at the interfacial site around the growth front of austenite. The inclusions entrapped by austenite make the interfacial site favourable for the chunky graphite nucleation but does not act as the nucleus substrate. Chunky graphite grows at the thin liquid channel in austenite. The growth front of the chunky graphite makes contact with the residual liquid iron through the thin liquid channel. The growth behaviour is similar to that of CV graphite.[24] The Mg gas bubble can be said to be the potential site for chunky graphite but it does not directly influence the nucleation and growth. As a free surface, the Mg gas bubble in liquid iron influences the graphite substructure. Once graphite takes on the growth behaviour of polycrystal substructure in the Mg gas bubble, it may never change its behaviour unless liquid iron suffers from harmful

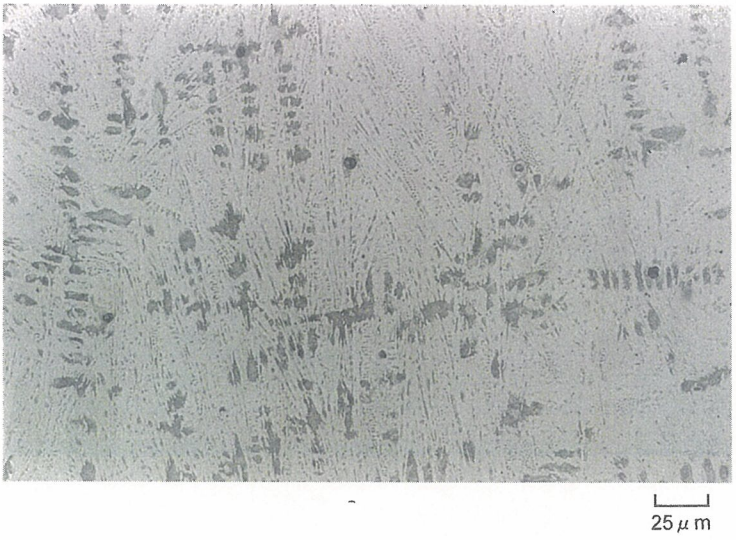

Fig. 6 Microstructure of sample quenched at point 1 in Figure 5 (5% nital etch)

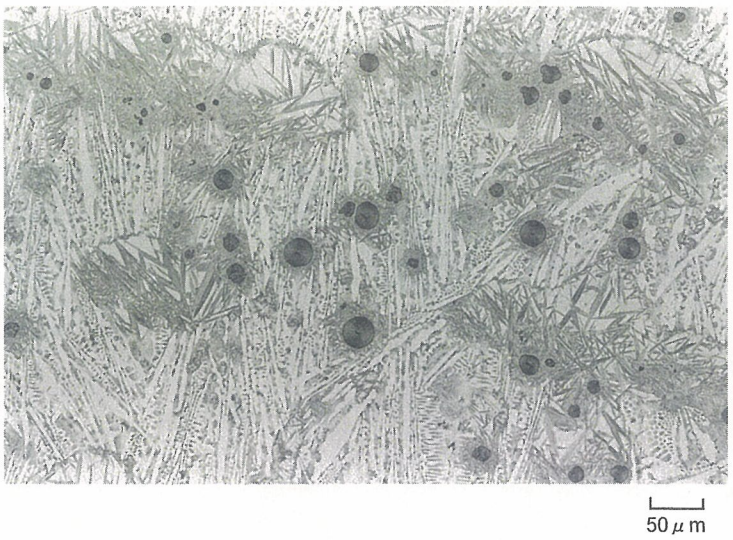

Fig. 7 Microstructure of sample quenched at point 2 in Figure 5 (5% nital etch)

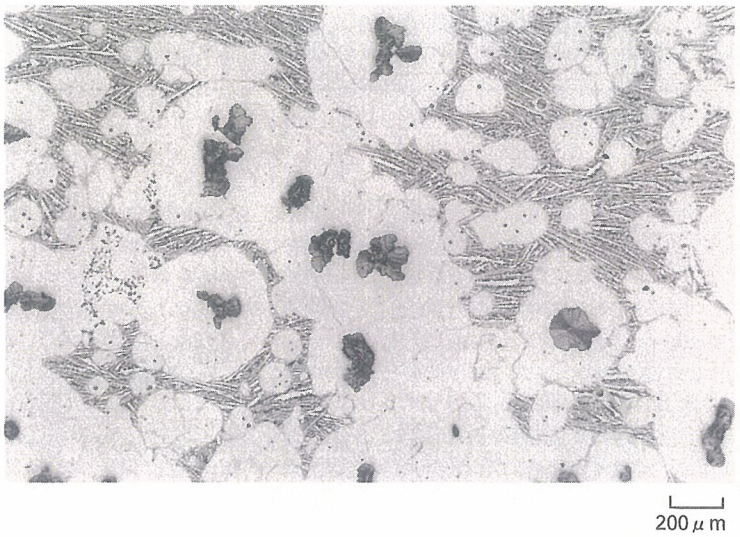

(a)

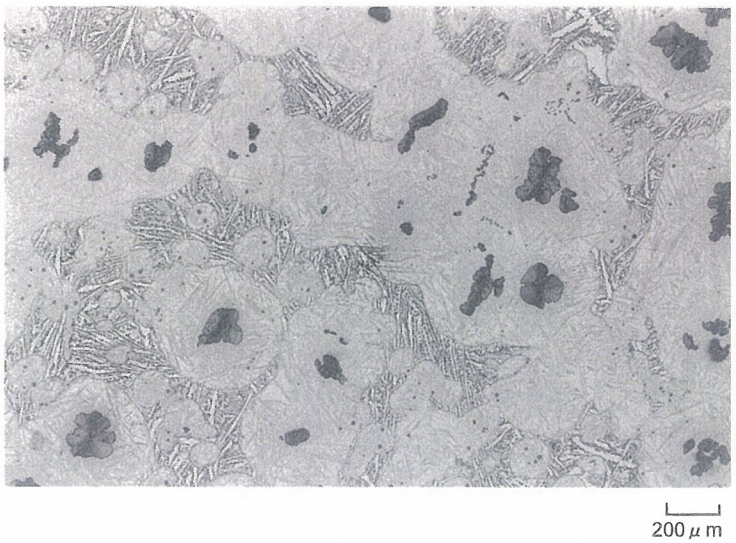

(b)

Fig. 8 Microstructures of sample quenched at point 3 in Figure 5 (5% nital etch)

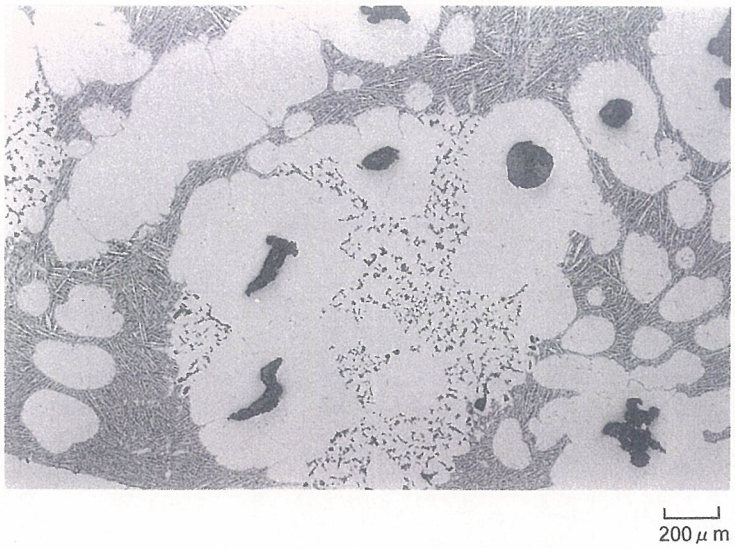

Fig. 9 Microstructures of sample quenched at point 4 in Figure 5 (5% nital etch)

Fig. 10 Growth front of chunky graphite making contact with residual liquid iron through liquid channel (5% nital etch). Sample was quenched at point 4 in Figure 5

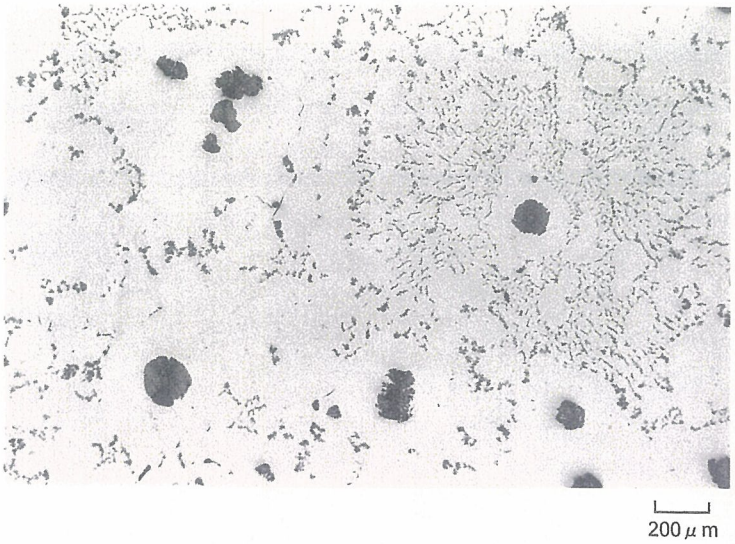

Fig. 11 Microstructure of sample solidified and cooled in SiC furnace (no etch)

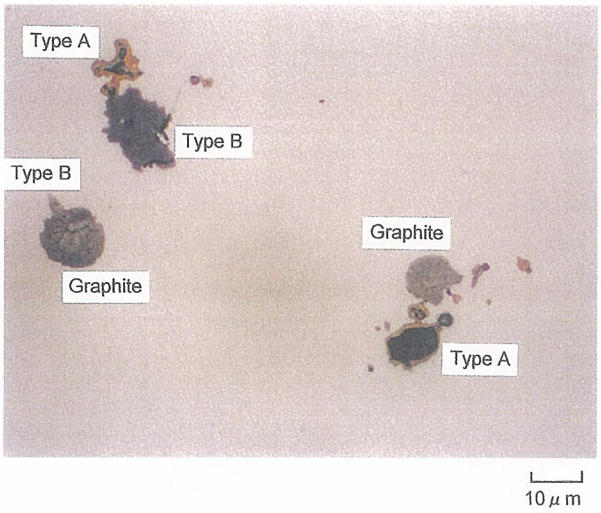

(a)

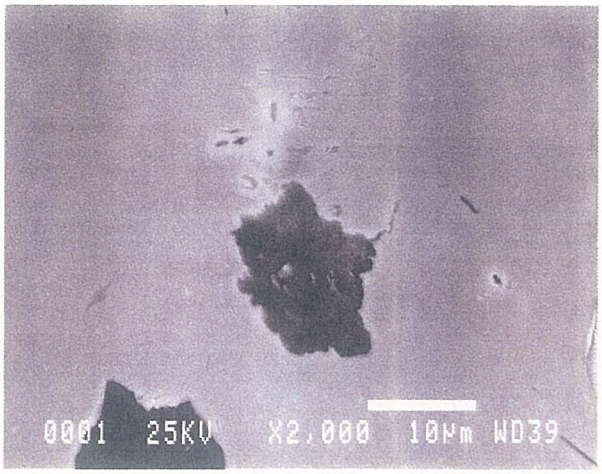

(b)

influences such as sulphur-attack by a furan-bonded sand mould. As a result, chunky graphite takes basically the same substructure as spheroidal and CV graphite.[22,23]

Cause of chunky graphite formation

Even if the condition of liquid iron after spheroidizing treatment is suitable to form a good spheroidal graphite structure, the final graphite morphology would not always be spheroidal. If the time duration from the magnesium treatment to the solidification start and the solidification time itself were too long, these conditions would reduce the number of graphite nodules and chunky graphite would form instead of the full spheroidal graphite structure. This could be because the effective number of Mg gas bubbles are lacking in liquid iron. The following possibilities are considered as the factors;

1 Mg gas bubbles may float out from liquid iron according to stoke's law.
2 Mg gas may change to liquid state by the eutectic expansion pressure (maximum $\fallingdotseq$ 60 atm[25]). In a laboratory, the liquid Mg droplets and the precipitation of chunky-like graphite has already been found by experience under high atmospheric pressure by B. Chang et al.[26]
3 Graphite may preferentially precipitate into the Mg gas bubble in the Si-rich region. However, even if the actual number is enough, the effective number might be reduced by the homogenisation of Si during the time duration.[27]

Fig. 12 Typical inclusions contacting with initial form of chunky graphite around growth front of austenite dendrite in specimen No. 3 (no etch); (a) optical photo and (b) SEM photo [inclusions at left-upper corner in photo (a)].

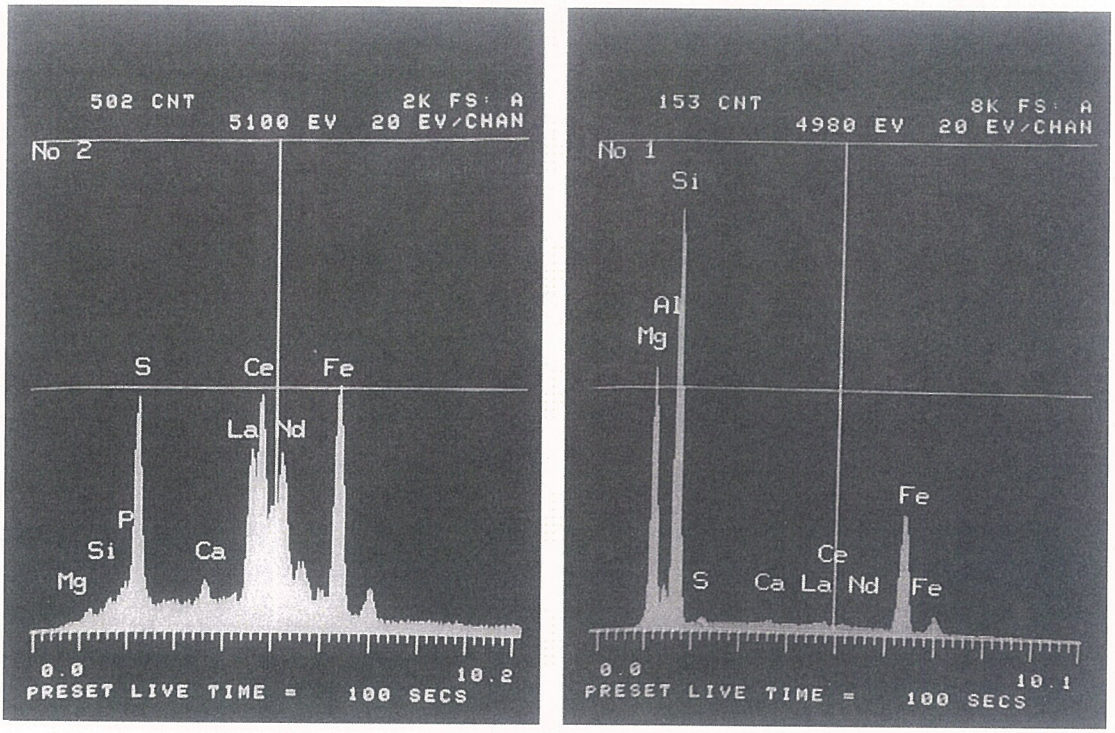

(a) (b)

Fig. 13 Results of EDS analysis on inclusions shown in Figure 12; (a) type A inclusion and (b) type B inclusion

4 Mg gas bubbles may collide with other floating particles such as inclusions and form a new inclusion. The Brownian Movement caused by the fluctuation of heat, element concentration, etc. may promote this.
5 When the temperature decreases, the diameter of the Mg gas bubble has to enlarge to keep the pressure balance between bubble and liquid iron. The gas bubble may enlarge its diameter through this collision promoted by the Brownian Movement.
6 In the case of Ni-resist ductile iron, Mg gas bubbles may react with Ni and form an intermetallic compound like $MgNi_2$ under the unequilbrium condition.

When there was a small number of sphere graphite nucleation sites, the growth of the graphite nodule stopped when the austenite shell became too thick. Then, the chunky graphite began to nucleate at some interfacial sites around the growth front of the austenite shell and dendrite. The Graphite nodule in the austenite shell is already isolated from the residual liquid iron at this point. These are the reason why the graphite formation by the diffusion of carbon and iron atoms would become easier at new interfacial sites than the pre-existing site in the thick austenite shell.

The elements such as Cu, Mo, Ni, Si, etc, widen the eutectic temperature range,[28] and promote the precipitation of chunky graphite by making the solidification longer.

Relationship with the precipitation of austenite dendrite

Although the chemical composition of liquid iron before solidification was hyper eutectic, austenite dendrite precipitated under conditions of chunky graphite formation. The reasons are considered to be that;

1 The floating-off of graphite dross leads residual liquid iron to the eutectic composition.
2 There may be a micro-area of hypo eutectic composition due to the negative segregation of Si in residual liquid iron even if the macro-analysis showed the eutectic composition.

Prevention of the chunky graphite formation in practice

According to the results of this experiment, the chunky graphite formation in heavy section ductile cast irons could be prevented by some well-grounded countermeasures. The most effective countermeasure must be the shortening of the solidification time by chillers. Good microstructure and mechanical properties could be obtained if the solidification time could be controlled within about 200 minutes, for example. At the same time, the time duration from the liquid treatment to the pouring start must be made as short as possible.

If there was a limitation on the above time, the other factors such as the super heating, the chemical composition, the post inoculation, the pouring temperature, etc. must be controlled. Since the practice is not always the same among foundries, the condition must be set for the individual foundry. The guide line is described below;

1 Super heating (°C, Min.) - - - - - - - - >1500, >5

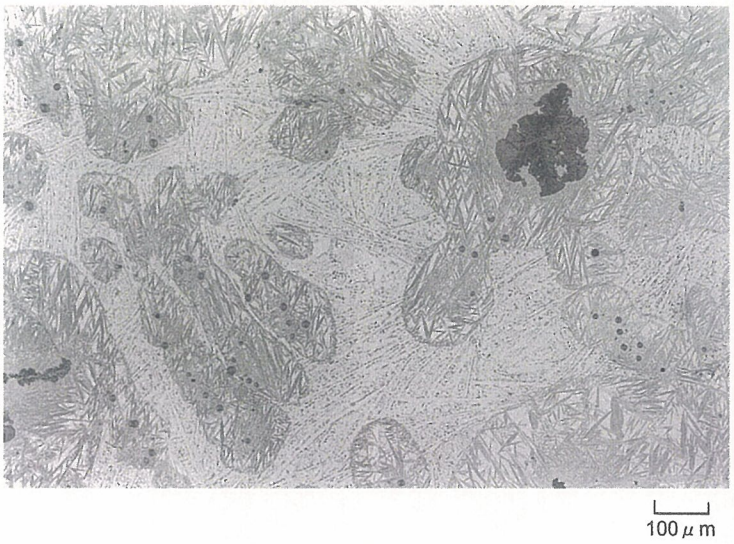

(a)

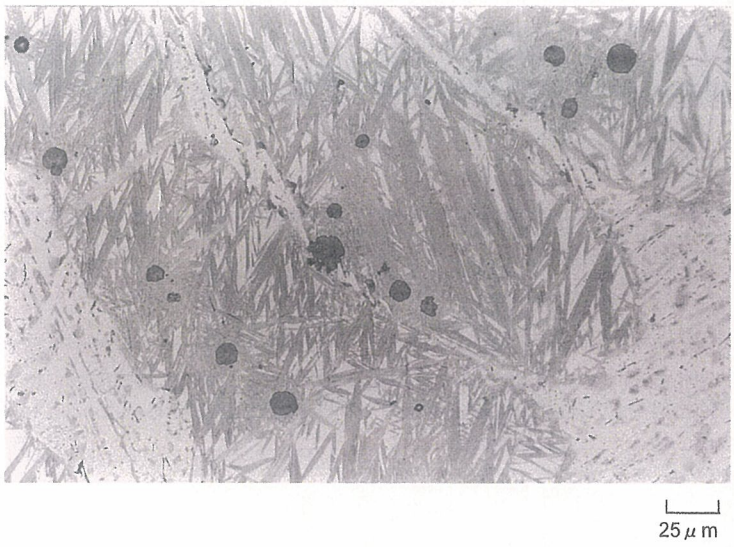

(b)

Fig. 14 Nucleation of chunky graphite at austenite-type A inclusion interface among austenite dendrite arms in sample No. 3 (5% nital etch); (a) low magnification under general light, (b) high magnification of (a), (c) the same magnification as (b) under polar light and (d) SEM of centre nodule with inclusion in (c)

2 Chemical composition (Mass%)

C 3.4–3.6	Ca <0.0030
Si 1.8–2.4	Ce stoichiometric amount to Al, As, Bi, Pb, Sb, Sn
Mn <0.35	Mg 0.040–0.050
P 0.030–0.040	CE 4.10–4.20
S 0.005–0.015	

3 Post inoculation (Mass%)- - -0.1

4 Pouring temperature (°C)- - - ΔT (over liquidus) = 100–150

However, if ductile iron needed to contain high silicon and/or alloy with Cu, Mo, Ni, etc. for a special material specification, such grades of ductile iron would be more sensitive to chunky graphite formation than non-alloyed ductile iron. A more drastic countermeasure is required for those kinds of ductile iron. Isolated materials such as a riser sleeve, riser neck, etc. would cause chunky graphite precipitation if they contained Al_2O_3 and metallic Al over a certain level.

Conclusion

The solidification behaviour of iron with chunky graphite was studied by observing the microstructure of samples quenched at some selected points during the solidification. The results were as follows:-

1 At the early stage of the solidification, only small graphite nodules under 10 μm (sphere graphite) directly precipitated in the liquid iron.

(c)

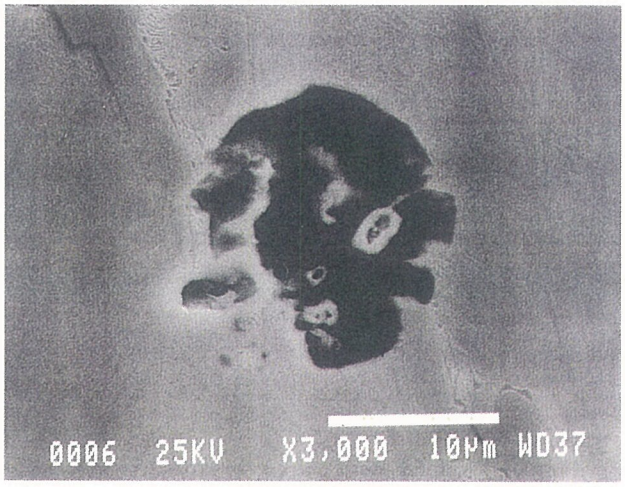

(d)

Fig 14 Continued

2 Sphere graphite grew into spheroidal graphite in the austenite shell but in small numbers compared with full nodule irons.
3 After the growth of spheroidal graphite stopped during solidification, chunky graphite nucleated at the interfacial site around the growth front of austenite.
4 There was no direct relationship between spheroidal and chunky graphite in terms of their nucleation and growth.
5 Chunky graphite grew along the liquid channel in austenite and the growth front came into contact with residual liquid iron through the channel.
6 A longer period of time between the spheroidizing treatment and the start of solidification and a longer solidification time promotes the nucleation of chunky graphite, reducing the number of nodules.

Acknowledgment

I am grateful to Managing Director Mr Hajime Yamada and secretary Ms Chiaki Takano in Ube Steel co., Ltd for all their help.

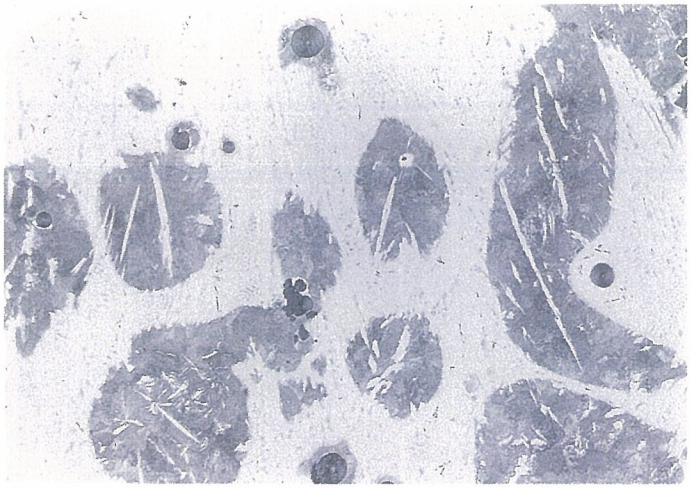

(a)

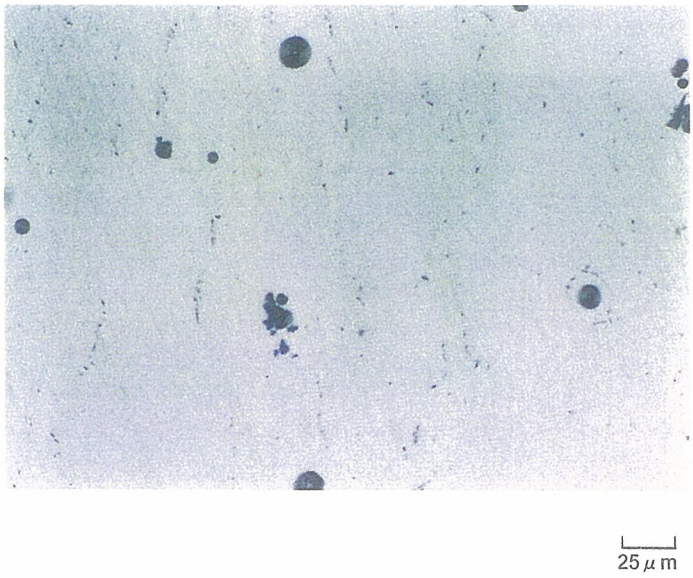

(b)

(c)

Fig. 15 Nucleation of chunky graphite at austenite-type B inclusion interface around austenite dendrite in sample No. 3; (a) general light (5% nital etch), (b) general light (no etch) and (c) polar light (no etch). These are all the same area

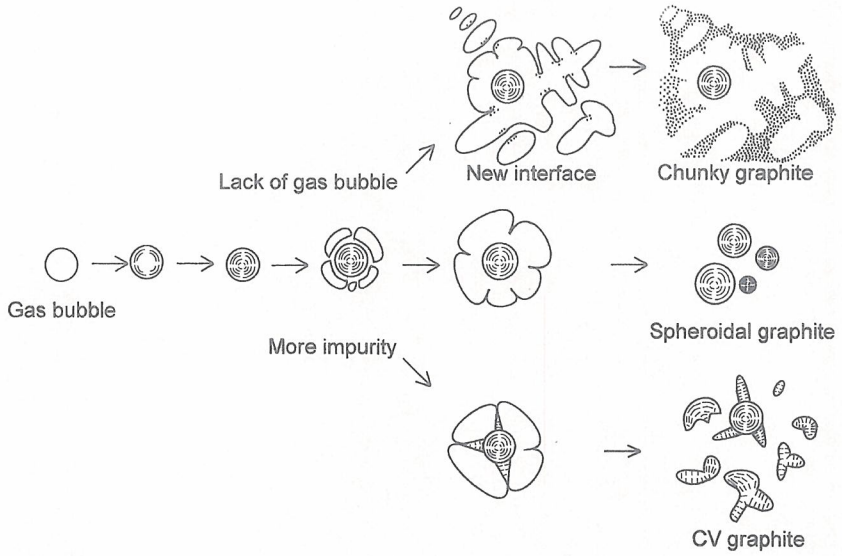

Fig. 16 Schematic illustration of graphite formation in liquid iron treated with spheroidizer

References

1. S. I. Karsay and R. D. Schelleng, ''Heavy Ductile Iron Castings Composition Effect on Graphite Structure,'' *Trans. AFS*, 1961, **69,** 672–679.
2. D. H. Wu, S. I. Karsay and R. D. Schelleng, ''Nickel Alloyed Austenitic Ductile Iron Graphite Structure,'' *Trans. AFS*, 1961, **69,** 725–730.
3. P. C. Liu, C. L. Li, D. H. Wu and C. R. Loper, Jr., ''SEM Study of Chunky Graphite in Heavy Section Ductile Iron,'' *Trans. AFS*, 1983, **91,** 119–126.
4. T. C. Xi, J. Fargues, M. Hecht and J. C. Margerie, ''The Formation and Prevention of Chunky Graphite in Slowly Solidified Non-alloy Spheroidal Irons,'' *Fonderie*, 1985, **46,** 14–23.
5. M. Gagne and D. Argo, ''*Heavy Section Ductile Iron Castings-Part 1; Structure and Properties*,'' ASM Int. Conf. on Casting, 1986.
6. N. Yingyi, Z. Zhu, ''A Study of the Rare Earth Effect on Chunky Graphite Formation in Heavy Section Ductile Iron,'' *Foundryman*, 1988, **81 No. 8,** 390–398.
7. B. Prinz, K. J. Reifferscheid, T. Schulze, R. Dopp and E. Schurmann, ''Investigation of Causes of Graphite Degenerations of SG Iron Like Chunky Graphite,'' *Giessereiforshung*, 1991, **43,** 3, 107–115.
8. S. I. Karsay and E. Campomanes, ''Control of Graphite Structure in Heavy Ductile Iron Castings,'' *Trans. AFS*, 1970, **78,** 85–92.
9. J. Zhou, W. Schmitz and S. Engler, ''Investigation of the Microstructure of Spheroidal Graphite Cast Iron for Low Solidification Rates,'' *Giessereiforschung*, 1987, **39,** No. 2, 55–70.
10. N. L. Church and R. D. Schelleng, ''Detrimental Effect of Calcium on Graphite Structure in Heavy Section Ductile Iron,'' *Trans. AFS*, 1970, **78,** 5–8.
11. C. Pelhan, I. Drganc and S. Spaic, ''Calcium in der Vorlegierung FeSiMg (Ca),'' *Giesserei-Praxis*, 1992, **17,** 247–254.
12. A. Jarvaid and C. R. Loper, Jr., ''Production of Heavy-Section Ductile Cast Iron,'' *AFS Trans.*, 1995, **103,** 135–150.
13. J. Zhou, W. Schmitz and S. Engler, ''State of Knowledge on the Microstructure in Spheroidal Graphite Cast Iron for Low Solidification Rates,'' *Giessereiforschung*, 1987, **39,** No. 2, 49–54.
14. R. K. Buhr, ''Vermiculite Graphite Formation in Heavy Section Nodular Iron Castings,'' *Trans. AFS*, 1968, **76,** 497–503.
15. R. K. Buhr, ''The Effect of Pb, Sb, Bi and Ce on Microstructure of Heavy Section Nodular Iron Castings,'' *Trans. AFS*, 1971, **79,** 247–252.
16. J. M. Greenhill, ''Some Practical Observations on Lead Contamination of Cast Iron,'' *Br. Foundryman*, 1984, **77,** No. 7, 370–378.
17. E. Campomanes, ''Effect of Minute Additions of Antimony on Structure and Properties of Ductile Iron,'' *Trans. AFS*, 1971, **79,** 57–62.
18. E. Campomanes, ''The Suppression of Graphite Deterioration in Heavy Section Ductile Iron Castings,'' *Giesserei*, 1978, **65,** No. 20, 535–540.
19. G. J. Cox, ''Untersuchung einer Moglichkeit zum Vermeiden von Chunky-Graphite in dickwandigen Gußstucken aus Austenitischen Gußeisen mit Kugelgraphit,'' *Giesserei-Praxis*, 1992, **18,** 274–276.
20. R. Barton, ''Production and Properties of Nodular Graphite Structure in Heavy Section Castings,'' *BCIRA J.*, Report 610, 1961, **9,** Sept., 668–686.
21. H. Itofuji, ''*Application of the Site Theory on the Quality Control of Heavy Section Spheroidal Graphite Cast Iron*,'' 1st Keith D. Millis World Symposium on Ductile Iron, Hilton Head Is., Sc, 1993.
22. H. Itofuji, et al., ''Comparison of Substructure of Compacted/Vermicular Graphite with Other Types of Graphite,'' *Trans. AFS*, 1983, **91,** 313–324.
23. H. Itofuji, ''Proposal of Site Theory,'' *AFS Trans.*, 1996, **104,** 79–87.
24. H. Itofuji, et al., ''The Formation Mechanism of Compacted/Vermicular Graphite in Cast Irons,'' *AFS Trans.*, 1983, **91,** 831–840.
25. K. S. Lee and N. Kayama, ''Pressure of Expansion of Cast Iron during Solidification,'' *IMONO*, 1975, **47,** No. 8, 11–16.
26. B. Chang, et al., ''*Spheroidal Graphite Cast Iron*,'' Agne Co., Ltd. Publish, 1983, 93–98.

27. H. Itofuji, et al., ''Formation Mechanism of Chunky Graphite in Heavy-Section Ductile Cast Irons,'' *Trans. AFS*, 1990, **98,** 429–448.
28. J. F. Janowak and R. B. Gundlach, ''A Modern Approach to Alloying Gray Iron,'' *Trans. AFS*, 1982, **90,** 847–863.

(Received 8 April 1999; accepted 15 August 2000)